Numerical Study on Convection Heat Transfer in Electro-Conductive Fluids by HSMAC Scheme

Hideo KAWAHARA* and Alexandru M. MOREGA**

Abstract

Convection of electrically conducting fluids such as liquid metals in the presence of magnetic field is a major area of investigation, e.g., crystal growth processes. The usage of a magnetic field is known to inhibit the thermal flow in the liquidus phase, and it is utilized in the design phase of casting systems. This study is concerned with the heat transfer and flow in electro-conductive melts in solidification systems. A mathematical model of the underlying physical processes is established, and numerical simulation results obtained by a home-made code based on the finite differences HSMAC scheme are reported: second order central finite differences for the viscous terms, third order up-wind (UTOPIA) finite differences for the convective terms, and first order forward finite differences for the time derivative.

Keywords: Electrically conducting fluids, Magnetic field, Heat transfer, HSMAC scheme,

Introduction

In the electromagnetic material processing, *e.g.*, crystal growth, solidification, laser melting, casting and vapor deposition, etc. [1-4] heat transfer plays a key role. In many circumstances, thermally driven flows in the melt are seen as menace for the processes, therefore, the knowledge and the control of convection heat transfer are important in obtaining high quality materials and in optimizing the fabrication technologies. Although extensive experimental studies are carried on to understand the role of convection heat transfer upon microstructures, the progress reported in the theory of natural and forced convection systems revolves mainly in the area of nonlinear dynamics, *e.g.* multiple solutions, periodic oscillations, chaos. On the other hand, there is a wide interest in developing numerical models aimed at understanding the solidification phenomena, as well as developing design tools usable in the optimization of fabrication technologies [1]. During crystal manufacturing, unwanted convective flows may be suppressed in liquid metals and other electrically conducting fluids by applying external magnetic fields. This technique is also successfully used in solidification processes to weaken the buoyancy driven flows and to modify the rate of solidification. Extensive studies were therefore conducted to examine the effect of magnetic field on the flow structure and stability of liquid metals [4-6].

Convection heat transfer with phase change solidification pose strongly nonlinear, coupled mathematical problems, characterized by abrupt changes in the temperature field that is particularly difficult to model numerically [7,8].

Magnetic field control in convection heat transfer solidification

The mathematical model

Figure 1,*a* shows a sketch of the physical domain for the problem under investigation. We focus on the transition from *liquidus* to *solidus* phase for a melted copper alloy, which is an electro-conductive, low Prandtl number viscous fluid. From the hydrodynamic point of view, the walls of the enclosure are no-slip. The top wall and bottom wall are isothermal (hot), at different temperature, and the outer wall is isothermal (cold). Two buffer rings separate the heater plates and the chiller. The fluid is permeated by an axial, uniform magnetic field $\boldsymbol{B} = \{0, B_{oz}\}$.

*商船学科 **Poliechnica University of Bucharest

2008 年 9 月 30 日受付

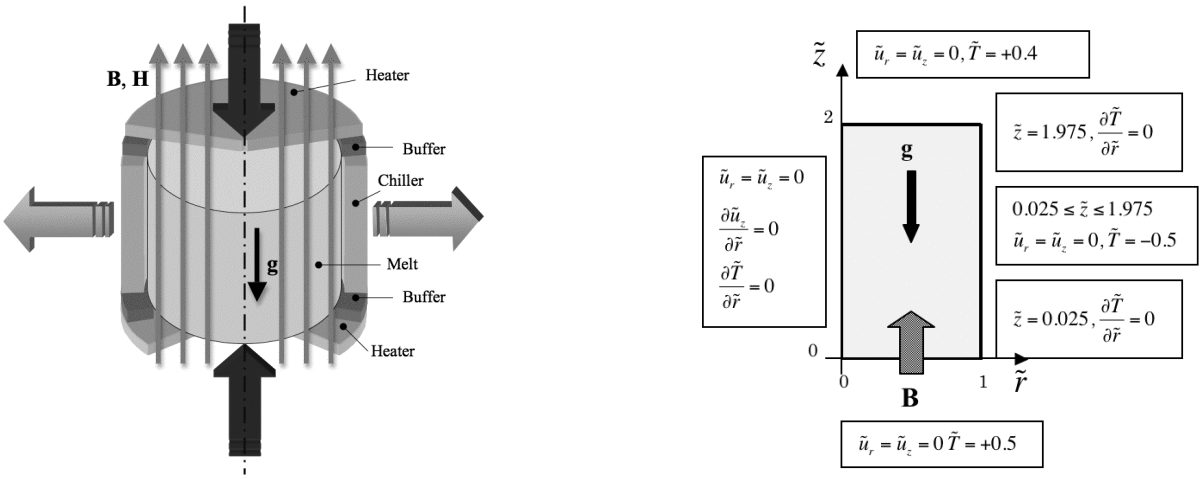

a. Physical system　　***b.*** Mathematical model; boundary conditions.

Fig. 1　Computational domain – cylindrical coordinates.

The working fluid is assumed to be Newtonian, Boussinesq, with constant properties, and its thermally driven flow is assumed laminar, incompressible [2].

Under these conditions, the thermally expansive fluid is subject to thermal gradients that generate a thermal flow. When an external magnetic field is superposed, the fluid is also siege of an induced electrical field [3]. In electro-conductive fluids (*e.g.*, melted metals), a non-negligible current field $\boldsymbol{J} = \sigma\left[\vec{\boldsymbol{v}} \times \boldsymbol{B}\right]$ is also present, giving rise to electro-dynamic, Lorentz body force; $\boldsymbol{v} = \{v_r, v_z\}$ is the velocity field, and σ is the electric conductivity of the fluid. This fundamental problem of thermal flow – magnetic field interaction provides insights in the mechanisms that may be used to control the system.

The mathematical model consists of the following non-dimensional equations

Momentum balance (*Navier-Stokes*)

$$\frac{\partial \tilde{\boldsymbol{v}}}{\partial \tau} + \left(\tilde{\boldsymbol{v}} \cdot \nabla\right)\tilde{\boldsymbol{v}} = -\nabla \tilde{p} + \mathrm{Pr}\nabla^2 \tilde{\boldsymbol{v}} + \mathrm{Ra} \cdot \mathrm{Pr}\,\theta \boldsymbol{e}_z \tag{1}$$

Mass balance

$$\nabla \cdot \tilde{\boldsymbol{v}} = 0 \tag{2}$$

Energy balance

$$\frac{\partial \theta}{\partial \tau} + \left(\tilde{\boldsymbol{v}} \cdot \nabla\right)\theta = \nabla^2 \theta \tag{3}$$

in the domain, $0 \le \tilde{r} \le 1$, $0 \le \tilde{z} \le A$ (A = cell height / cell radius = 2, is the cell aspect ratio). Here $\tilde{\boldsymbol{v}}$, θ, $\tilde{p}$, are non-dimensional velocity, temperature, and pressure fields. The scales for time, velocity, and pressure are L^2/ν, $U_0 = \alpha/L$ and $\rho\left(U_o/L\right)^2$, respectively. T is the dimensional temperature, the non-dimensional temperature is $\theta = \left(T - T_{melt}\right)/\left(T_h - T_c\right)$, and the magnetic field is scaled by B_0 (reference). The non-dimensional groups in eq. (1) are: Rayleigh number $\mathrm{Ra} = g\beta\left(T_h - T_c\right)L^3/\nu\alpha$; Hartmann number $Ha = B_{0z}L\sqrt{\sigma/\rho\nu}$; Prandtl number, $\mathrm{Pr} = \nu/\alpha$. Other quantities are: g – gravitational acceleration (in z-direction); β – thermal expansion coefficient; ν – kinematic viscosity; α – thermal diffusivity; ρ – mass density. The following initial and boundary conditions close the model

Initial conditions

$$\tau = 0: \begin{cases} \tilde{\boldsymbol{v}} = 0 \\ \theta = 0 \end{cases} \text{ for } 0 \le \tilde{r} \le 1,\ 0 \le \tilde{z} \le 2 \tag{4}$$

Boundary conditions

Horizontal bottom wall $(\tilde{z} = 0)$: $\tilde{\boldsymbol{v}} = 0$, $\theta = +0.5$.

Horizontal top wall $(\tilde{z} = A)$: $\tilde{\boldsymbol{v}} = 0$, $\theta = +0.4$.

Vertical inner wall $(\tilde{r} = 0)$: $\tilde{\boldsymbol{v}} = 0$, $\partial\theta/\partial\tilde{r} = 0$.

Vertical outer wall $(\tilde{r} = 1)$: $\tilde{\boldsymbol{v}} = 0$, $\theta = -0.5$.

The heat transfer rate, at the bottom wall, is given by the average Nusselt number

$$\overline{\mathrm{Nu}}\Big|_{z=0} = \int_0^1 \mathrm{Nu}\, \mathrm{d}r \qquad \mathrm{Nu} = -\frac{\partial\theta}{\partial\tilde{z}}\Big|_{\tilde{z}=0} \tag{5}$$

The numerical model – an HSMAC scheme

To solve the mathematical model we developed a home-made code based on the HSMAC method [8,9] that utilizes the finite differences approximation: second order central finite differences for the viscous terms, third order up-wind finite differences (UTOPIA) [10] for the convective terms, and first order forward finite differences for the time derivative. Accuracy tests indicate that 80×160 nodes, staggered, uniform grids provide grid-independent solutions.

We investigated thermal flows with Pr = 0.082, Ra = 1.64×10^9, and Ha = 0…100. The non-dimensional time step is $\Delta\tau = 1\times10^{-6}$. Details of the numerical algorithm are given next. The discrete form of eq. (1) is

$$\frac{{}^{m}(\tilde{v}_r)_{i,j}^{n+1} - {}^{m}(\tilde{v}_r)_{i,j}^{n}}{\Delta\tau} = \frac{{}^{m}(\tilde{p})_{i,j}^{n+1} - {}^{m}(\tilde{p})_{i+1,j}^{n+1}}{\Delta\tilde{r}} + (DSFR)_{i,j}^{n} \tag{6}$$

$$\frac{{}^{m}(\tilde{v}_z)_{i,j}^{n+1} - {}^{m}(\tilde{v}_z)_{i,j}^{n}}{\Delta\tau} = \frac{{}^{m}(\tilde{p})_{i,j}^{n+1} - {}^{m}(\tilde{p})_{i+1,j}^{n+1}}{\Delta\tilde{z}} + (DSFZ)_{i,j}^{n} \tag{7}$$

$$\frac{\theta_{i,j}^{n+1} - \theta_{i,j}^{n}}{\Delta\tau} = (DSEN)_{i,j}^{n} \tag{8}$$

Here *n* is the time step and *m* is the iteration index. *DSFR*, and *DSEN* stand for the convection and viscous terms. The grid nodes have the indices (*i*, *j*) in *r* and *z* directions, respectively.

The mass balance (2) provides an equation for pressure. Introducing the discrete derivative

$$D_{i,j}^{n+1} = \frac{(\tilde{v}_r)_{i,j}^{n+1} - (\tilde{v}_r)_{i-1,j}^{n+1}}{\Delta\tilde{r}} + \frac{(\tilde{v}_z)_{i,j}^{n+1} - (\tilde{v}_z)_{i,j-1}^{n+1}}{\Delta\tilde{z}} \tag{9}$$

the grid pressure $\tilde{p}_{i,j}$ may be calculated by Newton method

$$ {}^{m+1}\left(\tilde{p}\right)_{i,j}^{n+1} = {}^{m}\left(\tilde{p}\right)_{i,j}^{n+1} - {}^{m}D_{i,j}^{n+1}\left[{}^{m}\left(\frac{\partial D_{i,j}}{\partial \tilde{p}_{i,j}} \right)^{n+1} \right]^{-1} = {}^{m}\left(\tilde{p}\right)_{i,j}^{n+1} + \delta\left(\tilde{p}\right)_{i,j}^{n+1} \tag{10} $$

The velocity is given by

$$ {}^{m+1}\tilde{v}_{r,(i,j)}^{n+1} = {}^{m}\tilde{v}_{r,(i,j)}^{n+1} + \left(\frac{\partial \tilde{v}_{r,(i,j)}}{\partial \tilde{p}_{(i,j)}} \right)^{n+1} \delta\tilde{p}_{r,(i,j)}^{n+1} \tag{11} $$

$$ {}^{m+1}\tilde{v}_{z,(i,j)}^{n+1} = {}^{m}\tilde{v}_{z,(i,j)}^{n+1} + \left(\frac{\partial \tilde{v}_{z,(i,j)}}{\partial \tilde{p}_{(i,j)}} \right)^{n+1} \delta\tilde{p}_{z,(i,j)}^{n+1} \tag{12} $$

The calculation procedure is then:

1. Use eqs. (5), (6) to compute the velocities $\left\{ {}^{m+1}\left(\tilde{v}_r\right)_{i,j}^{n+1}, {}^{m+1}\left(\tilde{v}_z\right)_{i,j}^{n+1} \right\}$ for ${}^{m+1}\tilde{p}^{n+1} = {}^{m}\tilde{p}^{n}$.

2. Repeat the calculation until ${}^{m+1}D^{n+1} \le \varepsilon$ is satisfied, eq. (8)-(11) [in this study $\varepsilon = 10^{-3}$]; report $\left(\tilde{v}_r\right)^{n+1}$, $\left(\tilde{v}_z\right)^{n+1}$, $\tilde{p}^{n+1}$.

3. Calculate θ^{n+1} using eq. (7).

4. Repeat the cycle (1)-(3), until the final time.

Result and discussion

We analysed the effect of a magnetic field on the thermal flow by numerical simulation in the absence (Ha = 0), and in the presence of a magnetic field (Ha < 40). The fluid properties used in the numerical simulations are listed in Tab. 1.

Table 1 Heat transfers and flow properties of the model – copper alloy [11].

Quantity	*Liquidus*	*Solidus*
ρ [kg/m³]	8500	8500
C_p [J/mol·K]	530	380
k [W/m·K]	200	200
η [N·s/m²]	0.0434	·

Figure 2 shows the dynamics of the flow by Nu group, eq. (4), at the bottom wall. The initial, transient regime (τ =0…0.02) is discarded, and we focus on the oscillatory regimes that follow. Depending on Ha value, the frequency content and the amplitude of Nu is different.

Higher frequencies that appear may indicate either numerical noise or incipient turbulence. For Ha < 20 the dominant frequency of oscillation is low, and Ha–independent: *e.g.*, f = 629 for Ha = 0…~20. Further studies are needed to find the breaking point more accurately.

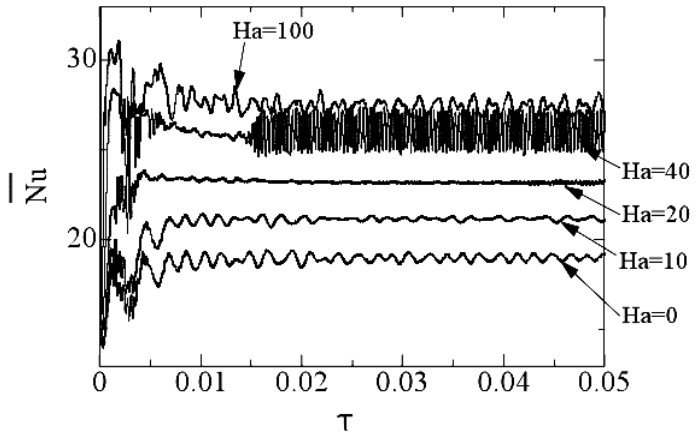

Fig. 2　Nu number at the bottom wall, for different Ha (non-dimensional time).

Figures 4, 5 evidence the periodic nature of the flow and the heat transfer for Ha = 0, at different time moments marked in Fig. 3.

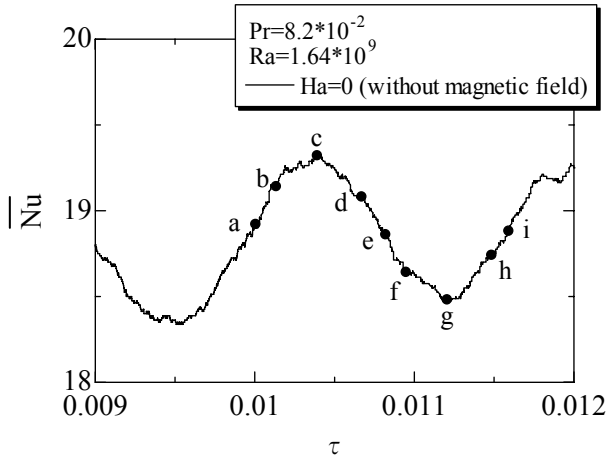

Fig. 3　The average Nu number at the bottom wall for Ha = 0.

A higher, dominant frequency (f = 2857) emerges about Ha = 20, where a change in the global dynamics is observable (see Fig. 4, where Ha = 40). This period-multiplication is accompanied by smooth decay and then increase of Nu amplitude with increasing Ha.

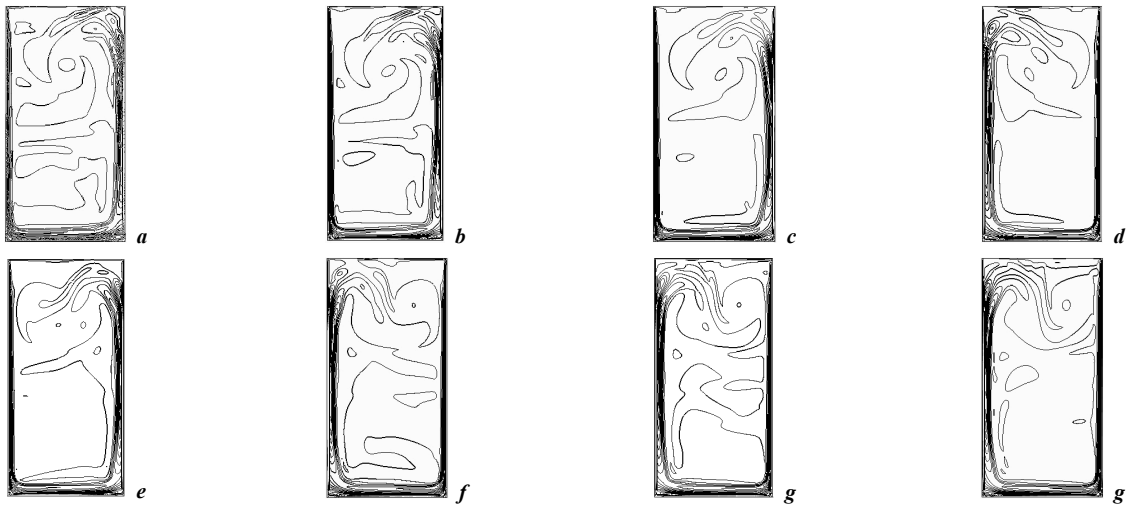

Fig. 4　Flow complexity and periodicity seen through streamlines.

Isotherms show regions of stable (lower part), and unstable thermal stratification (upper part).

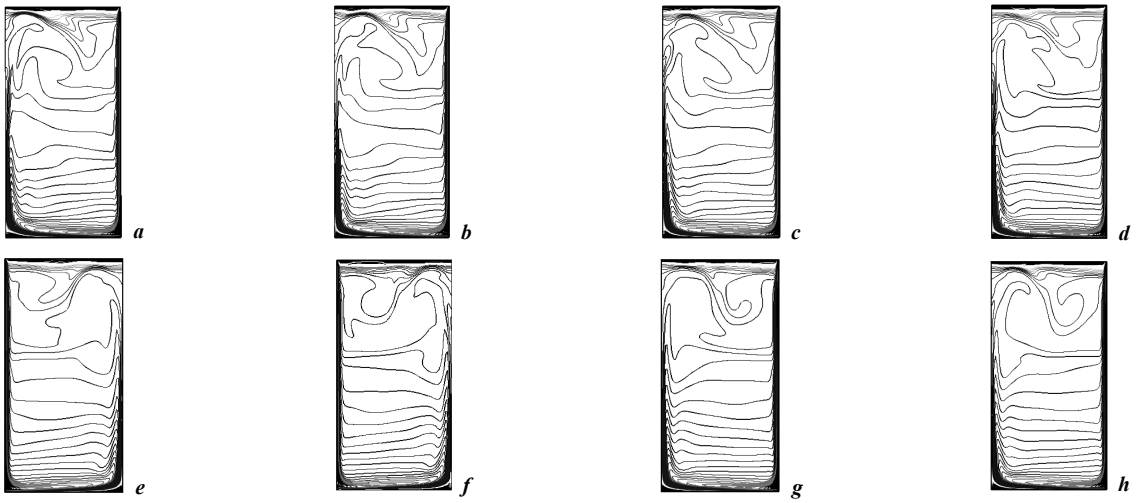

Fig. 5　Isotherms show regions of stable (bottom), and unstable thermal stratification (top).

For the selected aspect ration of the cell (A = 2), and the transfer conditions, the thermal flow is confined in the upper part of the cell (Fig. 4). On the other hand, the magnetic field in this study is axial therefore it acts upon (damps) the horizontal component of the flow.

Figure 7, 8 display the flow and heat transfer processes for Ha = 40, at different time moments marked in Fig. 6.

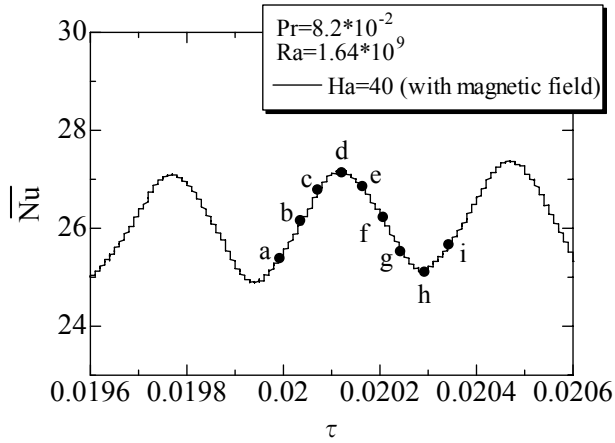

Fig. 6　The average Nu number at the bottom wall for Ha = 40.

High amplitude oscillations are now observed, and the thermal stratification in the bottom region of the cell is steeper. In fact, the flow is confined to the upper half of the cell.

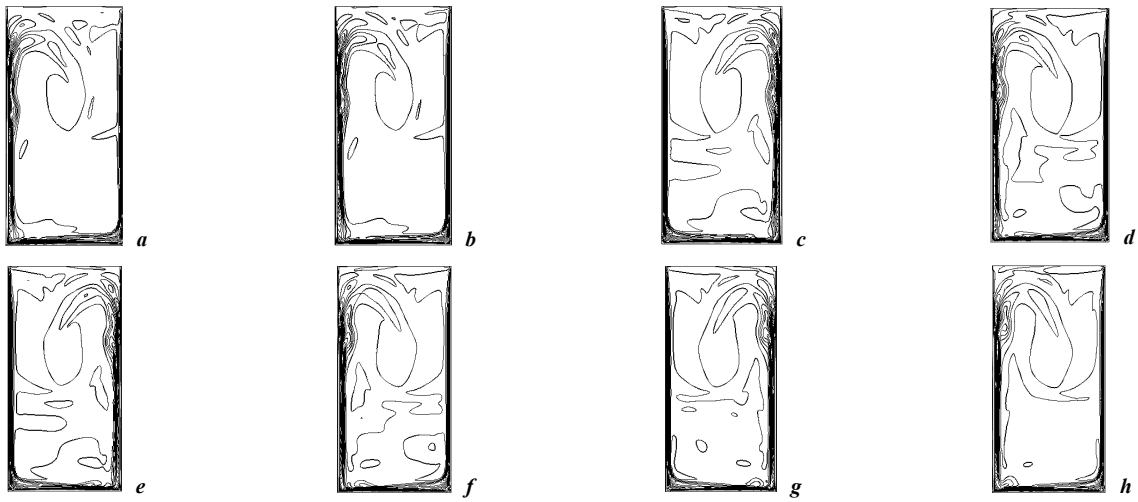

Fig. 7　Flow complexity and periodicity seen through streamlines.

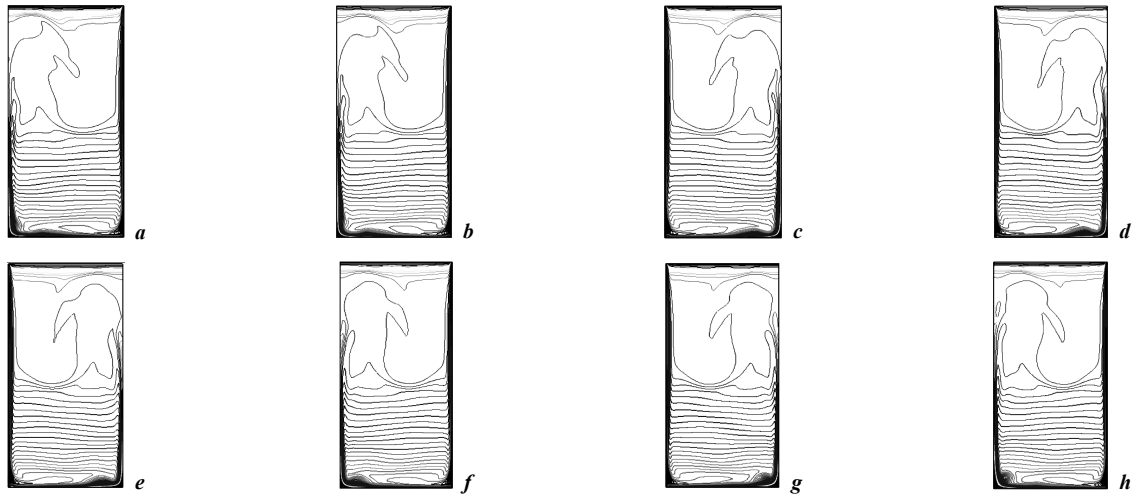

Fig. 8　Isotherms show regions of stable (bottom), and unstable thermal stratification (top).

Depending on the aspect ration of the cell (here, $A = 2$), its damping effect may vary. The vertical flow develops on a longer distance as compared to the horizontal flow. Since the magnetic field acts only on the horizontal component, its damping effect may be less effective. Further studies are needed to fully clarify the underlying mechanisms of this process of transition through period-multiplication.

Conclusions

In this study we investigated the heat transfer and flow field in the phase change solidification casting processes. The presence of a magnetic field results in Lorenz body forces, which may be used to modify the flow. The thermal flow is oscillatory. For Ha < 20 the dominant oscillation frequency is low, Ha–independent: *e.g.*, $f = 629$ (Ha = 0…~20). A higher frequency ($f = 2857$) emerges about Ha = 20, and a change in the global dynamics is observable. This period-multiplication is accompanied by smooth decay and then increase of Nu amplitude with increasing Ha. The aspect ratio of the cell and the heat transfer conditions and properties of the system are factors that may be utilized to influence the melt thermal flow – this study makes the object of future research.

References

[1] A.M Morega, T. Nishimura, *Combined heat and mass double-diffusive natural convection, ICHMT* Int. Symposium Transient convective heat and mass transfer in single and two-phase flows, TRCON-03, 17-22 August 2003, key lecture, Cesme, Turkey.

[2] T. Nishimura, A.M Morega, *Oscillatory natural convection by combined heat and mass transfer*, Trends Heat Mass & Momentum Transf., **6**, pp. 51-62 (2000).

[3] T. Nishimura, M. Wakamatsu, A.M. Morega, *Oscillatory double-diffusive convection in a rectangular enclosure with combined horizontal temperature and concentration gradients*, Int. J. Heat Mass Transfer, **41**, pp. 1601-1611 (1998).

[4] Moraru, A. Panaitescu, D. Mocanu, A.M Morega, I. Panaitescu, A. Soci, "Computational models for phenomena in aluminum electrolysis cells", *Rev. Roumaine Sci. Techn. Électrotech. et Énerg.*, **47**, 1, pp. 3-34 (2002).

[5] T. Tagawa, H. Ozoe, *Enhancement of heat transfer rate by application of a static magnetic field during natural convection of liquid metal in a cube*, J. Heat Transfer, **119**, pp. 265-271 (1997).

[6] A.M. Morega, *Magnetic field influence on the convective heat transfer in the solidification process*, Rev. Roum. Sci. Techn. Électrotechn. et Énerg., **33**, 1, Part I, pp. 33-39, Part II, 2, pp. 155-166 (1988).

[7] Bejan, *Convection heat transfer*, Wiley, NY (1984).

[8] R. Peyret, T.D. Taylor, *Computational methods for fluid flow, Springer Series in Computational Physics*, Springer Verlag, NY (1990).

[9] V.R.Voller, C.Prakash, *A Fixed Grid Numerical Modeling Methodology for Convection-Diffusion Mushy Region Phase Change Problem*s, Int. J. Heat Mass Transfer, **30**, pp. 1709-1719 (1987).

[10] T. Tagawa, H. Ozoe, "Enhancement of heat transfer rate by application of a static magnetic field during natural convection of liquid metal in a cube," *J. Heat Transfer*, **119**, 265-271, 1997.

[11] J. Fjellstedt, *Outokumpu Copper*, R&D, in [9].